IN-64
118027
P.30

NASA Contractor Report 189693
ICASE Report No. 92-38

ICASE

A BOUNDARY INTEGRAL METHOD FOR AN INVERSE PROBLEM IN THERMAL IMAGING

(NASA-CR-189693) A BOUNDARY INTEGRAL METHOD FOR AN INVERSE PROBLEM IN THERMAL IMAGING Final Report (ICASE) 30 p

N92-33006

Unclas

G3/64 0118027

Kurt Bryan

Contract Nos. NAS1-18605 and NAS1-19480
August 1992

Institute for Computer Applications in Science and Engineering
NASA Langley Research Center
Hampton, Virginia 23665-5225

Operated by the Universities Space Research Association

National Aeronautics and
Space Administration

Langley Research Center
Hampton, Virginia 23665-5225

A BOUNDARY INTEGRAL METHOD FOR AN INVERSE PROBLEM IN THERMAL IMAGING [1]

Kurt Bryan
Institute for Computer Applications in Science and Engineering
NASA Langley Research Center
Hampton, VA 23665

Abstract

This paper examines an inverse problem in thermal imaging, that of recovering a void in a material from its surface temperature response to external heating. Uniqueness and continuous dependence results for the inverse problem are demonstrated and a numerical method for its solution developed. This method is based on an optimization approach, coupled with a boundary integral equation formulation of the forward heat conduction problem. Some convergence results for the method are proved and several examples are presented using computationally generated data.

[1]This research was carried out while the author was in residence at the Institute for Computer Applications in Science and Engineering (ICASE), NASA Langley Research Center, Hampton, VA 23665, which is operated under National Aeronautics and Space Administration contracts NAS1-18605 and NAS1-19480.

1 Introduction

Thermal imaging is a technique of recent interest for the nondestructive evaluation of materials. This method attempts to characterize the internal structure of a sample (perhaps to locate flaws–disbonds, bubbles, corrosion, etc.) by using its surface temperature response to an external heating. Some recent work and techniques in this subject are detailed in [3], [4], [5], [7] and [9].

In this paper the problem of detecting and identifying an unknown internal void in a planar domain using thermal imaging is examined. The void could represent a defect in the material, or it could be a feature which is supposed to be present, e.g., a conduit, whose location or geometry is to be assessed. The focus is on the case in which the thermal stimulus, an applied heat flux at the boundary of the sample, is periodic. After separating the temporal and spatial variables, one obtains an inverse or domain identification problem for an elliptic equation. Results concerning the uniqueness and continuous dependence for the inverse problem will be examined and an algorithm for the numerical recovery of the void will be presented. This algorithm will be applied to examples using computationally generated data with and without noise.

The outline of the paper is as follows. Section 2 concerns the mathematical formulation of the forward heat conduction problem with periodic heating and demonstrates how this leads to an inverse problem for an elliptic equation. Section 3 contains an identification result for the inverse problem and shows that an internal void is determined by the boundary temperature response to external heating. This section also contains results concerning sensitivity or continuous dependence for estimates of the internal void based on the boundary measurements. These results rely on reformulating the heat conduction problem as an integral equation on the boundary of the sample. Section 4 examines a numerical method for the solution of the forward problem based on the boundary integral formulation and its incorporation into a least-squares routine for solution of the inverse problem. It is shown that with reasonable hypotheses on the class of voids, the numerical method will converge to the solution of the least-squares formulation of the inverse problem. Section 5 presents the results of this algorithm applied to computationally generated data.

2 Mathematical Formulation

The sample (without void) to be tested will be denoted by Ω, a bounded region in $\mathbb{R}^2$ with C^2 boundary. The internal void will be denoted by D, where $D \subset\subset \Omega$ with C^2 boundary. The function $\tilde{T}(t,x)$ will denote the solution to the heat equation

$$\begin{aligned} \frac{\partial \tilde{T}}{\partial t} - \kappa \triangle \tilde{T} &= 0 \text{ in } \Omega \setminus D \\ \alpha \frac{\partial \tilde{T}}{\partial \nu}|_{\partial\Omega} &= \tilde{g}(x,t) \\ \alpha \frac{\partial \tilde{T}}{\partial \nu}|_{\partial D} &= 0 \\ \tilde{T}(x,0) &= T_0(x) \end{aligned}$$

where ν is the outward unit normal vector field on the boundary of $\Omega \setminus D$, κ is the thermal diffusivity of Ω, α is the thermal conductivity of Ω, T_0 denotes the initial temperature of the region and $\tilde{g}$ is the heat flux at the boundary. Both κ and α are assumed to be known constants. Of course it is assumed that $\tilde{g}$ is not identically zero.

The heat flux $\tilde{g}(x,t)$ will be assumed to be periodic in time with known frequency $\frac{\omega}{2\pi}$ so that

$$\tilde{g}(x,t) = \mathrm{Re}\{e^{i\omega t} g(x)\}$$

for some complex valued function $g(x)$. Actually, $\tilde{g}$ would also generally include a steady-state term as well, but since only the periodic response is of interest, this term can be ignored. Under this assumption one can separate variables to find that $\tilde{T}(x,t) = \mathrm{Re}\{T(x)e^{i\omega t}\}$ where $T(x)$ satisfies

$$\begin{aligned} \triangle T - \frac{i\omega}{\kappa} T &= 0 \text{ in } \Omega \setminus D \\ \alpha \frac{\partial T}{\partial \nu}|_{\partial\Omega} &= g(x) \\ \alpha \frac{\partial T}{\partial \nu}|_{\partial D} &= 0, \end{aligned} \tag{2.1}$$

at least for time large enough so that the initial conditions do not matter. Note that the function $T(x)$ solving (2.1) will be complex-valued, consisting of a real, or in phase, and imaginary, or out of phase part.

The inverse problem of interest is the following: Given a known applied heat flux g, can the shape and location of the void D be uniquely determined from measurements of T on the boundary of Ω? Provided a uniqueness result holds, one would also like to know whether D depends continuously on measurements of T on $\partial\Omega$, that is, how sensitive estimates of D are to noise in the data. Finally, one would like an efficient computational algorithm for recovering an estimate of D from actual data.

3 The Inverse Problem

3.1 Uniqueness

A uniqueness result for the inverse problem follows easily from basic facts about elliptic operators.

Theorem 3.1 *(Uniqueness) Let D_1 and D_2 be two subdomains of Ω and T_1 and T_2 the corresponding solutions to equation (2.1) with nonzero Neumann data g. Let S be a portion of $\partial\Omega$ with positive measure. Then $T_1 \equiv T_2$ on S implies that $D_1 = D_2$.*

Proof: The functions T_1 and T_2 have the same Neumann data g and, since T_1 and T_2 agree on S, the same Cauchy data. Unique continuation for elliptic operators implies that T_1 and T_2 agree on $\Omega \setminus (D_1 \cup D_2)$. Then, for example, the function T_2 has a vanishing normal derivative on the region $D_1 \setminus D_2$, hence is constant on $D_1 \setminus D_2$. If $D_1 \setminus D_2 \neq \emptyset$ then by the maximum principle T_2 must be constant throughout $\Omega \setminus D_2$, contradicting $g \neq 0$. A similar argument shows that if $D_2 \setminus D_1 \neq \emptyset$ then T_1 would be constant on $\Omega \setminus D_1$, again contradicting $g \neq 0$, hence $D_1 = D_2$.

3.2 Boundary Integral Formulation

In order to investigate continuous dependence and numerical methods for the recovery of D it will convenient to reformulate the heat conduction problem as a boundary integral equation. This offers the advantage that one only has to solve for the temperature on the

boundary of the sample, rather than the interior. Since the boundary is the only place the temperature is measured, this is the only place its value is needed.

Use $\tilde{\Gamma}(r)$ to denote a fundamental solution or Green's function for the operator $(\triangle - \frac{i\omega}{\kappa})$. Such a fundamental solution is given by

$$\begin{aligned}\tilde{\Gamma}(r) &= -\frac{1}{2\pi} K_0(re^{i\pi/4}\sqrt{\omega/\kappa}) \\ &\equiv -\frac{1}{2\pi}(\ker(r\sqrt{\omega/\kappa}) + i\,\mathrm{kei}(r\sqrt{\omega/\kappa}))\end{aligned}$$

where K_0 is the zero order modified Bessel function of the second kind and ker and kei denote the kelvin functions. Efficient routines for computing the kelvin functions can be found in [1]. Define

$$\Gamma(x,y) = \tilde{\Gamma}(|x-y|).$$

The function Γ satisfies the heat equation in the y variable for fixed x, except at $x = y$, where it has a logarithmic singularity. Standard potential theory arguments (see [6], chapter 3) show that the elliptic problem given by equation (2.1) can be formulated as a boundary integral equation,

$$-\frac{1}{2}T(x) + \int_{\partial(\Omega\setminus D)} T(y)\partial_{\nu_y}\Gamma(x,y)\,dS_y = \int_{\partial(\Omega\setminus D)} \Gamma(x,y)g(y)\,dS_y \tag{3.1}$$

for each $x \in \partial(\Omega \setminus D)$ where ∂_{ν_y} is the normal derivative in the y variable and dS_y is surface measure. We will use $K(x,y)$ to denote the kernel $\partial_{\nu_y}\Gamma(x,y)$ for $x, y \in \partial(\Omega \setminus D)$ and use S to denote the operator

$$(S\phi)(x) = \int_{\partial(\Omega\setminus D)} K(x,y)\phi(y)\,dS_y. \tag{3.2}$$

The operator S is bounded and compact on $C(\partial(\Omega \setminus D))$, the space of continuous functions on $\partial(\Omega \setminus D)$, hence $-\frac{1}{2}I + S$ is a second kind Fredholm operator. Uniqueness of the solution to equation (3.1) follows from uniqueness of the solution to the forward problem. By the Fredholm alternative, the equation $(-\frac{1}{2}I + S)\phi = g$ is solvable, at least for smooth enough g. In particular, $(-\frac{1}{2} + S)^{-1}$ exists and is bounded on $C(\partial(\Omega \setminus D))$. The solution to equation (3.1) yields the temperature $T(x)$ on $\partial\Omega$ and ∂D. If needed, the temperature for $x \in \Omega \setminus D$ can be found from the relation (Green's third identity)

$$T(x) = \int_{\partial(\Omega\setminus D)} (T(y)\partial_{\nu_y}\Gamma(x,y) - \Gamma(x,y)g(y))\,dS_y.$$

3.3 Restrictions on the Domain

In order to obtain continuous dependence results, a few restrictions on the class of voids and their parameterization are needed. First, let us use $\tilde{C}^2[0,1]$ to denote the space of C^2 functions on $[0,1]$ where the endpoints 0 and 1 are identified with each other. This space can be normed by $\|\phi\| = \sup_{t\in[0,1]} |D^\beta \phi|$, $|\beta| \leq 2$. We assume that D depends on finitely many parameters, $D = D(q)$ with $q \in Q \subset\subset \mathbb{R}^m$ and where:

(a) $q_1 = q_2$ implies $D(q_1) = D(q_2)$ (unique parameterization).

(b) $D(q) \subset \Omega' \subset\subset \Omega$ for $q \in Q$ ($D(q)$ stays away from $\partial\Omega$).

(c) The closed curves $\partial D(q)$ are parameterized as $x(q,t) = (x_1(q,t), x_2(q,t))$ for $q \in Q$, $0 \leq t < 1$, with $x_i(q,t)$ a $\tilde{C}^2$ function of t for each $q \in Q$ and $\frac{dS}{dt} = \sqrt{(x_1')^2 + (x_2')^2}$ bounded away from zero. Also, the map $q \to x(q,t)$ is continuous from $\mathbb{R}^m$ to $\tilde{C}^2[0,1]$. Based on the above assumptions it is not difficult to show that:

(d) For each $x \in \partial D(q)$ there exists an open ball, $B_\epsilon(x)$, of radius ϵ around x with ϵ independent of x and q such that the curve $\partial D(q) \cap B_\epsilon(x)$ is parameterized by $(x_1(q,t), x_2(q,t))$ with t in some connected interval.

The continuity of $q \to \tilde{C}^2$ and compactness of Q imply that the $\tilde{C}^2$ norm of $x(q,t)$ as a function of t is uniformly bounded over $q \in Q$. Also, for $q \in Q$ the families of functions $x(q,t)$, $x'(q,t)$ and $x''(q,t)$ are equicontinuous in t, where the prime denotes differentiation with respect to t.

Lemma 3.1 *The family of functions $\{K(x(q,s), x(q,t));\ q \in Q\}$, are (uniformly) equicontinuous in s and t, that is, for each $\epsilon > 0$ there is a $\delta > 0$ so that*

$$|K(x(q,s), x(q,t)) - K(x(q,s'), x(q,t'))| \leq \epsilon$$

for all (s,t) and (s',t') with

$$|s - s'| \leq \delta, \quad |t - t'| \leq \delta,$$

and δ does not depend on s, t or q.

Proof: For brevity let us suppress the dependence of $x()$ and $K()$ on q and write simply $K(s,t)$ for $K(x(s),x(t))$. Also, since $\Gamma(x,y) = \log(|x-y|) + G(x,y)$ where G is smooth in x and y, we will prove the lemma assuming that $\Gamma(x,y) = \log(|x-y|)$; it is easy to check that the smooth term makes no difference in the proof.

The stated regularity for K holds on the compact set $\{(s,t) \in [0,1] \times [0,1],\ \ |s-t| \geq \epsilon,\ q \in Q\}$, where ϵ is any number greater than zero, for on this set K is at least C^2. We need only to show that $K(s,t)$ is uniformly continuous on the set $(s,t) \in [0,1] \times [0,1]$, $|s-t| \leq \epsilon$.

Suppose the boundary of D near a point x_0 is parameterized by $x(t) = (x_1(t), x_2(t))$. By making an appropriate translation and rotation it may be assumed that $x_0 = x(0) = (0,0)$ and that the boundary is oriented so that the unit normal outward vector in (x_1, x_2) coordinates is $(0,1)$. In this case Taylor's theorem can be used to expand $x(t)$ as

$$\begin{aligned} x_1(t) &= a_0 t + \frac{a_1}{2}t^2 + R_1(t) \\ x_2(t) &= \frac{b}{2}t^2 + R_2(t) \end{aligned}$$

where

$$\begin{aligned} a_0 &= x_1'(0) \\ a_1 &= x_1''(0) \\ b &= x_2''(0) \\ R_j(t) &= \frac{1}{2}(x_j''(c) - x_j''(0))t^2, \quad j = 1,2, \end{aligned}$$

and c is some point between 0 and t. The functions R_1 and R_2 are functions whose $\tilde{C}^2$ norms can be bounded in terms of the norms of x_1 and x_2. The unit normal vectors satisfy

$$\begin{aligned} \nu_1(t)\frac{dS}{dt} &= x_2'(t) = bt + R_2'(t) \\ \nu_2(t)\frac{dS}{dt} &= -x_1'(t) = -a_0 - a_1 t - R_1'(t). \end{aligned}$$

The kernel $K(s,t)$ is then given by

$$\begin{aligned} \partial_{\nu_y}\Gamma(x(s),x(t))\frac{dS}{dt} &= \frac{1}{2\pi}\frac{(x_1(s)-x_1(t))\nu_1(t) + (x_2(s)-x_2(t))\nu_2(t))}{(x_1(s)-x_1(t))^2 + (x_2(s)-x_2(t))^2}\frac{dS}{dt} \\ &= \frac{1}{2\pi}\frac{(x_1(s)-x_1(t))x_2'(t) - (x_2(s)-x_2(t))x_1'(t))}{(x_1(s)-x_1(t))^2 + (x_2(s)-x_2(t))^2}. \end{aligned} \tag{3.3}$$

Substituting the above expressions for x_1, x_2, x_1' and x_2' gives for the numerator, after some simplification,

$$num = -\frac{a_0 b}{2}(s-t)^2 + R_2'(t)(s-t)\left[a_0 + \frac{a_1}{2}(s+t)\right] + [R_1(s) - R_1(t)](bt + R_2'(t)) \\ -(R_2(s) - R_2(t))\left[a_0 + a_1 t + R_1'(t)\right] - \frac{b}{2}(s^2 - t^2)R_1'(t).$$

The denominator becomes 2π times

$$\left[a_0(t-s) + \frac{a_1}{2}(s^2 - t^2) + R_1(s) - R_1(t)\right]^2 + \left[\frac{b}{2}(s^2 - t^2) + R_2(t)\right]^2$$

Taylor's theorem implies that

$$R_j(s) = R_j(t) + (s-t)R_j'(t) + \frac{1}{2}(s-t)^2 R_j''(c)$$

for some point c between s and t. Substituting this into the expression for the numerator gives

$$num = \frac{(s-t)^2}{2}\left[-a_0 b + (bt + R_2'(t))R_1''(c) - (a_0 + a_1 t + R_1'(t))R_2''(\tilde{c}) + a_1 R_2'(t) - bR_1'(t)\right]$$

where c and $\tilde{c}$ are between s and t. Doing the same for the denominator shows

$$den = 2\pi(s-t)^2\left[(a_0 + R_1'(t))^2 + (R_2'(t))^2 + C_1 s + C_2 t\right]$$

where C_1 and C_2 are functions of s and t which can be bounded in terms of the $\tilde{C}^2$ norm of $x(t)$. Cancelling the common $(s-t)^2$ factor, the kernel can be written as

$$K(s,t) = \frac{1}{4\pi}\frac{-a_0 b + [bt + R_2'(t)]R_1''(c) - [a_0 - a_1 t - R_1'(t)]R_2''(\tilde{c}) + a_1 R_2'(t) - bR_1'(t)}{[a_0 + R_1'(t)]^2 + [R_2'(t)]^2 + C_1 s + C_2 t} \quad (3.4)$$

Since $R_1'(0) = 0$, the kernel is bounded through $s = t$, for the denominator is bounded away from zero for s and t in a sufficiently small neighborhood of zero. In fact, by Taylor's theorem $R_1'(t) = R_1'(0) + R_1''(c)t = R_1''(c)t$ for some c between zero and t. In addition, since the functions C_1 and C_2 can be bounded in terms of the $\tilde{C}^2$ norm of $x(t)$ (which is itself bounded uniformly over Q), the denominator may be bounded uniformly away from zero for s and t in a neighborhood of 0, with the neighborhood and bound independent of x_0 and q. The families of functions $x_j'(t)$ and $x_j''(t)$, as well as $R_j'(t)$ and $R_j''(t)$, are uniformly equicontinuous for $q \in Q$, and hence so are both the numerator and denominator of equation

(3.4). Since the denominator of $K(s,t)$ is bounded away from zero, it follows that the family of functions $\{K(x(q,s),x(q,t));\ q \in Q\}$ is uniformly equicontinuous in s and t. ■

By parameterizing $\partial D(q)$ with $x(t)$, $0 \le t < 1$ as above and parameterizing $\partial\Omega$ with $x(t)$, $1 \le t < 2$, one can identify the boundary of $\partial(\Omega \setminus D)$ with the fixed interval $[0,2)$. A solution $T(x)$ to equation (3.1) can be identified with a function $T(t)$ on $[0,2)$ by $T(t) = T(x(t))$. For a function ϕ defined on $[0,2)$ let ϕ_1 and ϕ_2 denote the restriction of ϕ to $[0,1)$ and $[1,2)$, respectively. We will work in the space of functions ϕ for which ϕ_1 is continuous and extends continuously to $[0,1]$ with $\phi_1(0) = \phi_1(1)$ and for which ϕ_2 is continuous and extends continuously to $[1,2]$ with $\phi_2(1) = \phi_2(2)$. We will denote this space by $\tilde{C}[0,2]$ and norm it with the supremum norm. The solutions $T(t)$ to (3.1) lie in this space. One can also identify the operator S (a function of q) with an integral operator on $\tilde{C}[0,2]$. Let us write $K(q,s,t)$ instead of $K(x(q,s),x(q,t))$ and define

$$S(q)\phi(s) = \int_0^2 K(q,s,t)\phi(t)\frac{dS}{dt}\,dt. \tag{3.5}$$

The same argument given in the proof of Lemma 3.1 shows that $K(q,s,t)$ is uniformly equicontinuous for s and t in $[1,2)$, i.e., for $x(s)$ and $x(t)$ on the boundary of Ω and $q \in Q$, (actually, K here is independent of q). For $s \in [0,1)$ and $t \in [1,2)$ (or vice-versa) $K(q,s,t)$ is C^2 in s and t, since in this case $x(s) \in \partial D$, $x(t) \in \partial\Omega$ and by assumption the boundaries do not intersect, so again $K(q,s,t)$ is uniformly equicontinuous over $q \in Q$. The kernel K will have a jump discontinuity at $s = 1$ or $t = 1$, since there $x(t)$ jumps from ∂D to $\partial\Omega$. In summary, the family of functions $\{K(q,s,t);\ q \in Q\}$, is uniformly equicontinuous on $[p,p+1) \times [q,q+1)$ $p,q = 1,2$, with simple jump discontinuities at $s = 1$ or $t = 1$.

Another fact worth noting is that the map $q \to K(q,s,t)$ is continuous as a map from $\mathbb{R}^m$ to $\tilde{C}[0,2] \times \tilde{C}[0,2]$, that is, for any $\epsilon > 0$ there is a δ so that $|q - \tilde{q}| \le \delta$ implies

$$\sup_{s,t\in[0,2]} |K(q,s,t) - K(\tilde{q},s,t| \le \epsilon.$$

This follows directly from equation (3.4) and the fact that $q \to x_j'(q,t)$, $q \to x_j''(q,t)$, $q \to R_j'(t)$ and $q \to R_j''(t)$ are all continuous as maps from $\mathbb{R}^m$ to the space of continuous functions.

3.4 Continuous Dependence

Based on the above assumptions it is possible to prove a version of continuous dependence.

Theorem 3.2 *Let q_n be a sequence in Q and $T(q_n)$ the corresponding solution to equation (2.1) with $D = D(q_n)$. Suppose $T(q_n) \to T(q^*)$ in $C(\partial(\Omega \setminus D))$ for some $q^* \in Q$. Then $q_n \to q^*$.*

Proof: The first task is to show that the map $q \to S(q)$ is continuous. Let $S_1 = S(q)$ denote the boundary integral operator for $D = D(q)$ (considered as an operator on $\tilde{C}[0,2]$) and $S_2 = S(q + \delta q)$, where $q \in Q$ and δq is some small perturbation in q. As remarked above, $q \to K(q,s,t)$ is continuous. It follows that $q \to S(q)$ is also continuous as a map from $\mathbb{R}^m$ to the space of operators on $\tilde{C}[0,2]$, for if $|K(q+\delta q,s,t) - K(q,s,t)| \leq \epsilon$ for all $s,t \in [0,2]$ then

$$\begin{aligned} \|(S_2\phi)(s) - (S_1\phi)(s)\| &\leq \int_0^2 |K(q+\delta q,s,t) - K(q,s,t)||\phi(t)|\,dt \\ &\leq C\epsilon\|\phi\|, \end{aligned}$$

for some constant C, that is, $\|S(q+\delta q) - S(q)\| \leq C\epsilon$ for δq sufficiently small.

The next step is to show that $q \to (I - S(q))^{-1}$ is continuous. The operator $(-\frac{1}{2}I + S_1)$ is invertible and $(-\frac{1}{2}I + S_2)$ can be inverted with a Neumann series as follows. First note that

$$\begin{aligned} (-\frac{1}{2}I + S_2)^{-1} &= (-\frac{1}{2}I + S_1 - (S_1 - S_2))^{-1} \\ &= (-\frac{1}{2}I + S_1)^{-1}(I + (-\frac{1}{2}I + S_1)(S_1 - S_2))^{-1}. \end{aligned}$$

Let $R = -(-\frac{1}{2}I + S_1)(S_1 - S_2))$. Given any $\epsilon > 0$ one can choose a $|\delta q|$ sufficiently small so that $\|R\| \leq \epsilon$ and, for $\epsilon < 1$,

$$\begin{aligned} (-\frac{1}{2}I + S_2)^{-1} &= (-\frac{1}{2}I + S_1)^{-1}(I + R)^{-1} \\ &= (-\frac{1}{2}I + S_1)^{-1}(I + R + R^2 + \cdots) \end{aligned}$$

so that

$$(-\frac{1}{2}I + S_2)^{-1} - (-\frac{1}{2}I + S_1)^{-1} = R + R^2 + \cdots$$

and

$$\|(-\frac{1}{2}I + S_1)^{-1} - (-\frac{1}{2}I + S_2)^{-1}\| \leq \frac{\|R\|}{1 - \|R\|} \tag{3.6}$$

$$\leq \frac{\epsilon}{1 - \epsilon}. \tag{3.7}$$

Thus the map $q \to (-\frac{1}{2}I + S(q))^{-1}$ is continuous and so the map $q \to T(q) = (-\frac{1}{2} + S(q))^{-1}g$ is continuous from $\mathbb{R}^m$ to $\tilde{C}[0,2]$.

To complete the proof, suppose that the sequence q_n does not converge to q^*. Since Q is compact, some subsequence of q_n converges to some $\tilde{q} \in Q$. It can be assumed that this is simply the sequence q_n. However, continuity of $q \to T(q)$ means that $T(q_n) \to T(\tilde{q})$, implying $T(q^*) = T(\tilde{q})$ and contradicting the uniqueness Theorem 3.1.

4 Numerical Methods

4.1 Nyström's Method

The following computational approach to the inverse problem is based on a least-squares formulation, finding the model void parameters which best fit the measured data by means of an optimization method. One drawback to this approach is the need to repeatedly solve the heat conduction problem (2.1). It is thus advantageous to have an efficient method for solving this equation. The boundary integral equation approach is such a method, and in this section we examine a technique for its solution.

The boundary integral formulation (3.1) for the solution T to equation (2.1) can be written

$$-\frac{1}{2}T(s) + \int_0^2 K(s,t)T(t)\,dt = g(s) \tag{4.1}$$

where $T(s)$ means $T(x(s))$ for the parameterization $x(s)$ of $\partial(\Omega \setminus D)$. Surface measure $\frac{dS}{dt}$ has been included in the kernel K. Let t_j and ω_j $j = 1, \cdots, n$ denote the nodes and weights of a quadrature rule convergent on the space $\tilde{C}[0,2]$, so that

$$\sum_{j=1}^{n} \omega_j f(t_j) \approx \int_0^2 f(t)\,dt$$

if $f(t)$ is smooth enough. Actually, we will consider a family of quadrature rules, indexed by n, with

$$\lim_{n\to\infty} \sum_{j=1}^{n} \omega_j f(t_j) = \int_0^2 f(t)\,dt$$

for continuous f, e.g., the n-node composite trapezoidal rule. We will also assume that the quadrature rule converges uniformly over any set $\mathcal{F}$ of equicontinuous functions in $\tilde{C}[0,2]$, so that if $f \in \mathcal{F}$,

$$\left| \int_0^2 f(t)\,dt - \sum_{j=1}^{n} \omega_j f(t_j) \right| \leq \epsilon$$

for $n \geq N(\epsilon)$, $N(\epsilon)$ independent of f. The n-node trapezoidal rule is an example of such a family, or more appropriately, the trapezoidal rule applied separately to each interval $[0,1]$, $[1,2]$.

Nyström's method consists of replacing the integral in equation (4.1) with the quadrature rule to obtain

$$-\frac{1}{2}T_n(s) + \sum_{j=1}^{n} K(s,t_j)\omega_j T_n(t_j) = g(s). \tag{4.2}$$

Now let $s = t_1, t_2, \cdots$ to obtain the $n \times n$ linear system

$$-\frac{1}{2}T_n(t_i) + \sum_{j=1}^{n} K(t_i,t_j)\omega_j T_n(t_j) = g(t_i). \tag{4.3}$$

The idea is that $T_n(t_i) \approx T(t_i)$. As shown in [2], each solution to equation (4.2) leads to a solution to equation (4.3) and moreover, each solution to equation (4.3) corresponds to a unique solution to equation (4.2) with which it agrees at the nodes $t_1, \cdots, t_n$. Equation (4.3) is the system which is solved numerically although (4.2) is the equation we will use for the error analysis.

Write equations (4.1) and (4.2) as

$$\begin{aligned} (-\frac{1}{2}I + S)T &= g \\ (-\frac{1}{2}I + S_n)T_n &= g \end{aligned}$$

where S_n is the operator in equation (4.2). Note that S_n is compact since it is a finite rank operator on $\tilde{C}[0,2]$. Recall that S and S_n depend on the parameter q.

Theorem 4.1 *$T_n \to T$ in $\tilde{C}[0,2]$ as $n \to \infty$. The convergence is uniform over $q \in Q$.*

In proving this theorem the following result will be useful. It can be found in [2], section 3.0.

Theorem 4.2 *Let X be a Banach space, let S and $(\lambda - S)^{-1}$ be bounded linear operators on X, with $\lambda \neq 0$. Let T be a bounded linear operator on X with the property that either λ is an eigenvalue of T or $(\lambda - T)^{-1}$ exists (if T is compact, this is satisfied). Further, assume*

$$\|(T-S)T\| < \frac{\lambda}{\|(\lambda - S)^{-1}\|}.$$

Then $(\lambda - T)^{-1}$ exists on X and

$$\|(\lambda - T)^{-1}\| \leq \frac{1 + \|(\lambda - S)^{-1}\|\|T\|}{|\lambda| - \|(\lambda - S)^{-1}\|\|(T-S)T\|}.$$

Furthermore, if $(\lambda - S)f = g$ and $(\lambda - T)h = g$ then

$$\|f - h\| \leq \|(\lambda - S)^{-1}\| \frac{\|(T-S)T\|\|f\| + \|(T-S)g\|}{|\lambda| - \|(\lambda - S)^{-1}\|\|(T-S)T\|}.$$

Proof of Theorem 4.1 The proof of Theorem 4.1 is simply an application of Theorem 4.2 with $X = \tilde{C}[0,2]$, $\lambda = -1/2$, $S = -S$ and $T = -S_n$. In the previous section it was shown that the map $q \to (-\frac{1}{2}I + S(q))^{-1}$ is continuous, hence $\| - \frac{1}{2}I + S(q))^{-1}\|$ can be uniformly bounded over Q. In order to complete the proof of Theorem 4.1 it must be shown that

$$\|(S - S_n)S_n\| \rightarrow 0 \tag{4.4}$$

$$\|(S - S_n)g\| \rightarrow 0 \tag{4.5}$$

as $n \to \infty$, uniformly for $q \in Q$. This, in conjunction with Theorem 4.2, will show that $\|T - T_n\| \to 0$ uniformly in q.

From the argument given in section 3, for $s \in [0,2]$ and $q \in Q$, the kernel $K(q,s,t)$ is uniformly equicontinuous in the t variable. The uniform convergence of $\|(S - S_n)g\|$ to zero follows from

$$\begin{aligned}(S - S_n)g(s) &= \int_0^2 (K(s,t)g(t)\,dt - \sum_{j=1}^{n} K(s,t_j)\omega_j g(t_j) \\ &\leq \epsilon(n)\end{aligned}$$

with $\epsilon(n) \to 0$ as $n \to \infty$, independently of q and s. Here we have used the fact that K is equicontinuous in t and the assumption that the integration rule converges uniformly over equicontinuous sets in $\tilde{C}[0,2]$.

The case for the convergence of $\|(S - S_n)S_n\|$ is similar. Let ϕ be a function in $\tilde{C}[0,2]$ with $\|\phi\| = 1$. Since K is uniformly equicontinuous in s and t,

$$\begin{aligned} S_n\phi(s+\Delta s) - S_n\phi(s) &= \sum_{j=1}^{n}(K(s+\Delta s, t_j) - K(s,t_j))\omega_j\phi(t_j) \\ &\leq \epsilon(\Delta s)\|\phi\|\sum_{j=1}^{n}|\omega_j| \end{aligned}$$

where $\epsilon(\Delta s)$ does not depend on s, t or q. For convergent integration rules the sum $\sum_{j=1}^{n}|\omega_j|$ is bounded in n (see [2], part I, section 4, theorem 7), so that $S_n\phi$ is an equicontinuous function, independent of q. The rest of the argument is as in the previous paragraph but with g replaced by $S_n\phi$. This shows that $\|(S - S_n)S_n\| \to 0$ uniformly for $q \in Q$ and completes the proof of Theorem 4.1.

4.2 Application to Inverse Problem

Let us suppose that the temperature data for the inverse problem consists of point measurements T_i at points x_i on the boundary of Ω, $i = 1, \cdots, M$. A reasonable way to attempt a recovery of the unknown region D is to define the functional

$$J(q) = \sum_{i=1}^{M}(T(q)(x_i) - T_i)^2$$

and seek an estimate of $D(q)$ as the solution to

(IDP) $\qquad$ minimize $J(q)$ for $q \in Q$

In practice the solution to this problem will involve not the true temperature $T(q)$, but the n-node Nyström approximation $T_n(q)$. The actual minimization problem solved will be

(IDP)^n $\qquad$ minimize $J^n(q)$ for $q \in Q$

where

$$J^n(q) = \sum_{i=1}^{M}(T_n(q)(x_i) - T_i)^2. \tag{4.6}$$

Based on the analysis of the convergence of T_n to T, the following theorem can be stated.

Theorem 4.3 *Let q_n be a solution to (IDP)^n. Then as $n \to \infty$, some subsequence of q_n converges to $q^* \in Q$. Moreover, q^* is a solution to (IDP).*

Note that if the boundary data T_i are consistent with some $D(q^*)$ for $q^* \in Q$ then, since there is a unique such q^*, one can talk about the unique solution to (IDP) and a subsequence of q_n will converge to this q^*.

Proof of Theorem 4.3: Some subsequence of q_n converges to a point $q^* \in Q$ by virtue of the fact that Q is compact. Let q_m be any sequence in Q converging to q^*. From the uniform convergence of T_n to T over Q we can conclude that

$$\lim_{m,n\to\infty} J^n(q_m) = J(q^*). \tag{4.7}$$

For any $q \in Q$ we have

$$J^n(q_n) \leq J^n(q).$$

Taking the limit over n and using (4.7) shows that

$$J(q^*) \leq J(q)$$

for all $q \in Q$, i.e., q^* solves (IDP).

5 Implementation and Examples

5.1 Introduction

In this section the recovery algorithm is implemented and the results of some numerical experiments are described. One modification is made to the assumptions of the previous sections: for experimental work it is more convenient to use a sample Ω which is rectangular, thus the boundary of Ω will not be C^2. This make little difference to the integral equation formulation, for the operator $(I - S(q))$, while no longer a second kind Fredholm operator, is in fact a small perturbation of such an operator. One can still establish the existence and boundedness of the inverse $(I - S(q))^{-1}$; see [10] for more details. The rest of the arguments are unchanged. The solution T on the boundary of Ω is still continuous, although it will have

"corners" at the corresponding corners of Ω. For numerical purposes it is thus beneficial to use a quadrature rule which allocates more nodes near these corners, rather than uniformly over the boundary of Ω. Note that it is still assumed that ∂D is C^2.

One other modification will also be made: The heat flux g will be a point heating source, so that $g(x) = \delta_P$, a delta function, where P is the point at which the heat is applied. While this flux g does not live in the space of functions in which we have been working, as will be shown one can analytically remove the singularity from the problem and work with a smooth remainder term which fits the hypotheses made so far. In the examples that follow we use only the imaginary or out of phase portion of the periodic temperature response T. This part of the temperature is continuous, even through the singularity at the point heating source. The real or in phase part of T, however, has a logarithmic singularity at the point source. In reality one does not have a point source, but for a heat source concentrated in a small region the in phase response in the region of the source varies radically with the heat source "footprint", which causes problems in a reconstruction algorithm. In practice therefore, one excludes the in phase data near the source. For convenience, we simply work only with the out of phase portion.

One final remark: The linear system obtained via the n-node Nyström's method can be written

$$A(q)T_n(q) = f(q) \tag{5.1}$$

where $A(q)$ is the matrix generated by the discretization and $b(q)$ is the right hand side of the discretized integral equation; both depend on the parameter q which defines the void. As a result, the temperature T_n also depends on q. The Levenberg-Marquardt optimization routine used requires the derivatives of the functional $J(q)$ with respect to q which in turn requires $\frac{\partial T_n}{\partial q}$. On can obtain these derivatives by differentiating equation (5.1) with respect to q to obtain

$$A(q)\frac{\partial T_n}{\partial q} = \frac{\partial f}{\partial q} - \frac{\partial A}{\partial q}T_n(q). \tag{5.2}$$

Both $A(q)$ and $f(q)$ are differentiable with respect to q and if $A(q)$ is not singular then the above computation is valid, that is, $\frac{\partial T_n}{\partial q}$ exists and therefore satisfies equation (5.2). Once T_n has been obtained, $\frac{\partial T_n}{\partial q}$ can be obtained from (5.2); in fact, the work done in solving the equation (LU decomposition) can be re-used in computing the derivative. It should be noted

that the temperature satisfies equation (5.2) at both the finite-dimensional (matrix) level and infinite dimensional (integral equation) level, i.e., $\frac{\partial T}{\partial q}$ also exists.

5.2 Sample Geometry and Implementation

The geometry used for the examples is illustrated in Figure 1. The lower left corner of the rectangular sample has (x_1, x_2) coordinates $(0, 0)$. We will examine the case where the voids are disks of unknown center and radius, $D = D(q)$ with $q = (a, b, r)$ where (a, b) is the center of the disk in (x_1, x_2) coordinates and r is the radius. The boundary of D is parameterized by $x_1(t) = a + r\cos(2\pi t)$, $x_2(t) = b + r\sin(2\pi t)$, $0 \leq t < 1$. If the length (x_1 axis) of Ω is L

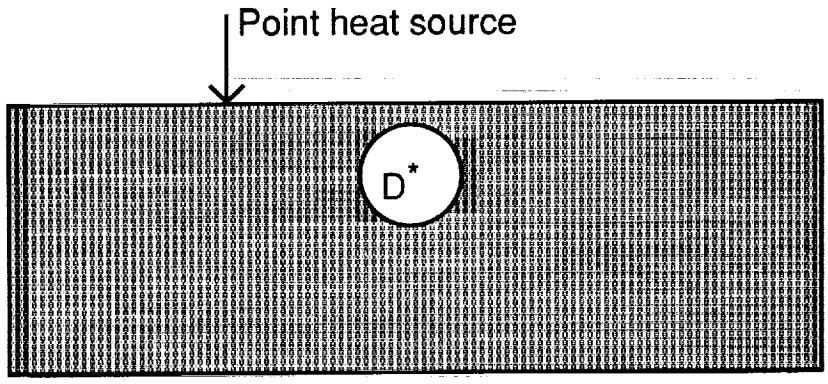

Figure 1: Sample geometry.

and the height (x_2 axis) is H then the boundary of Ω is parameterized from $t = 1$ to $t = 2$ by

$$f(x) = \begin{cases} (4Lt, 0) & 1 \leq t < \frac{5}{4} \\ (L, 4H(t - \frac{5}{4})) & \frac{5}{4} \leq t < \frac{3}{2} \\ (L - (t - \frac{3}{2}), H) & \frac{3}{2} \leq t < \frac{7}{4} \\ (0, H - 4H(t - \frac{7}{4})) & \frac{7}{4} \leq t < 2. \end{cases}$$

With appropriate bounds on the range of a, b and r, it is simple to check that this class of voids and parameterization satisfies the properties of section 3. The dimensions of the sample

for the present example will be 1.27 cm in length by 0.32 cm in height. All references to coordinates and sample geometry will be in centimeters. The thermal parameters correspond to aluminum. As mentioned above, the heat flux will be a point source applied at a points with (x_1, x_2) coordinates (x_1, 0.32 cm) on the top of the sample. This source will have unit (one watt) power. Note that for the full time-dependent problem this means that the *variation* in heat flux is one watt.

The quadrature rule used for Nystöm's method for the solution of equation (3.1) is just a version of the midpoint or trapezoidal rule with variably spaced nodes. Specifically, let $f(x) = 2^{p-1}x^p$ for $0 \leq x \leq \frac{1}{2}$. The variable p is a parameter to adjust the spacing of the nodes. Allocate N nodes t_i (N even) and weights w_i on the interval $[0,1]$ by

$$t_i = \begin{cases} f(\frac{i-1/2}{N}), & i = 1, \ldots, \frac{N}{2} \\ 1 - t_{N-i+1}, & i = \frac{N}{2}+1, \ldots, N \end{cases}$$

The corresponding weights are

$$w_i = \begin{cases} \frac{1}{2}(t_1 + t_2), & i = 1 \\ \frac{1}{2}(t_{i+1} - t_{i-1}), & i = 2, \ldots, N \\ 1 - \frac{1}{2}(t_{N-1} + t_N), & i = N. \end{cases}$$

This rule allocates nodes and weights to $(0,1)$, excluding the endpoints. For $p = 1$ it is just the midpoint rule on $[0,1]$. Choosing $p > 1$ causes the nodes to "bunch up" near 0 and 1. For each of the four sides of $\partial\Omega$ the nodes are allocated by mapping the above nodes on $[0,1]$ to the corresponding interval in t, e.g., the nodes are allocated on the bottom of Ω by transforming the nodes on $[0,1]$ as $t \rightarrow \frac{t}{4} + 1$ with the corresponding change in the weights. The parameter p is chosen to be 2.0; this allocates more nodes close to the corners of Ω. On the void boundary ∂D the nodes are evenly spaced with weights corresponding to the trapezoidal rule on $[0,1]$. The typical number of nodes used is 10 to 30 on each side of Ω and 20 to 40 on the void boundary.

In order to deal with the singular boundary heating, first note that if $\Gamma(x,y)$ is a fundamental solution to $L = (\triangle - \frac{i\omega}{\kappa})$ then $L_y\Gamma(x,y) = 0$ for $y \neq x$, where L_y means the operator

applied in the y variable Moreover, if $P \in \partial\Omega$ and $\tilde{T}(y) = -2\Gamma(P,y)/\alpha$ then it can be shown that

$$\alpha\partial_{\nu_y}\tilde{T}(y) = \delta_P - 2\partial_{\nu_y}\Gamma(P,y) \quad \text{on} \quad \partial\Omega,$$

that is, for delta function heating $\tilde{T}$ is the solution up to a nonsingular remainder term. The remainder term on the right hand side is actually continuous on $\partial\Omega$, or, more precisely, extends continuously through $y = P$. Thus one can analytically remove the singularity associated with the point heating and simply solve for the smoother remainder term. The forward heat conduction problem for the example is then

$$\begin{aligned} (\triangle - \frac{i\omega}{\kappa})T &= 0 \quad \text{in} \quad \Omega \setminus D \\ \alpha\partial_\nu T &= 2\partial_{\nu_y}\Gamma(P,y) \quad \text{on} \quad \partial(\Omega \setminus D). \end{aligned} \tag{5.3}$$

The full solution with delta function heat flux would be given by the sum $T(y) + \tilde{T}(y)$. This solution has a logarithmic singularity in its real part and has smooth imaginary part.

For reconstruction purposes, the temperature in the present examples will only be measured along the top of the sample, so that the least squares fit functional (4.6) includes only this data. The heating frequency is in the range of 1 to 5 Hz. For each heating source the temperature response is measured at 40 equispaced points along the top of the sample.

5.3 Strategy

One of the necessities of an optimization approach is that one have a reasonable initial guess at the true void before beginning the optimization procedure, or else risk become trapped in a local minimum far from the "true" solution. This is particularly applicable in the present case, as illustrated by the following figures. The sample with void is shown in Figure 2. The sample is again aluminum with the same dimensions as in Figure 1. The true void D^* (solid outline) has a radius of 0.06 cm and is centered at (x_1, x_2) coordinates (0.88 cm, 0.24 cm). The heat source is applied directly on top of D^* at 3 Hertz. The prospective void D is fixed to have the same radius and x_2 coordinate as D^*; its x_1 coordinate is allowed to vary from 0.15 cm to 1.15 cm. The value of the functional $J(q)$ as a function of x_1 is shown in Figure 3. The functional is of course zero when the x_1 coordinates of D and D^* coincide and the

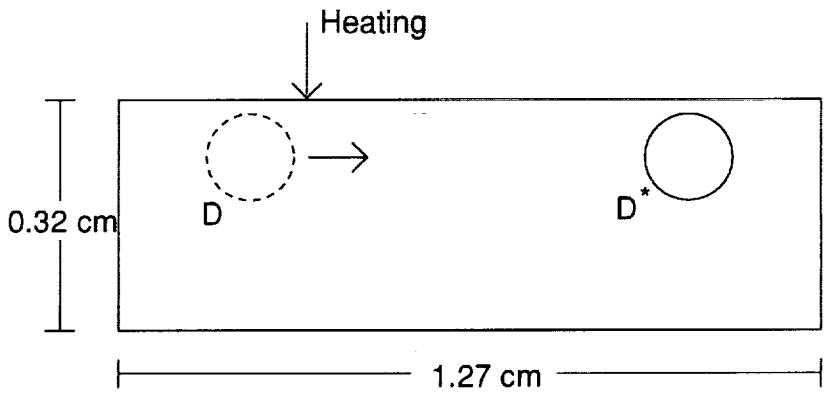

Figure 2: Sample geometry for least-squares functional example.

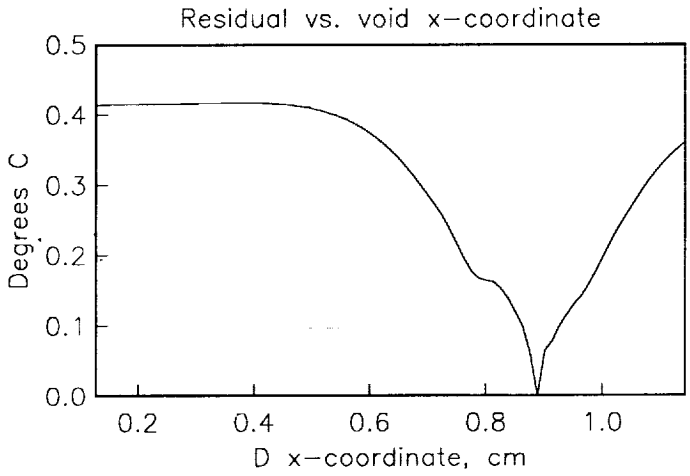

Figure 3: Functional $J(q)$ versus D x_1 coordinate.

functional rises steeply as one moves away from the minimum. However, if one used an optimization method with an initial guess which was far from the correct value ($x_1 < 0.5$ cm) then the optimization routine would probably not be successful, for in this region the functional is almost flat–actually, it slopes slightly away from the minimum. This illustrates the need for a reasonable initial guess at the x_1 coordinate of the void D^*.

In the previous example the heat source was applied directly on top of the true void D^*. In reality if a single heat source is applied it will not likely fall on top of or even near

D^*. Figure 4 illustrates the same situation as Figures 2 and 3 but with the heat source far (x_1 coordinate 0.35 cm) from D^*. Here the situation is even worse, for now the least-squares functional has many local minima to trap any optimization method started with an x_1 coordinate far from D^*. Also, since the heat source does not "illuminate" D^*, the functional is very flat near the minimum. In the presence of noise one would not be able to locate this minimum with any accuracy.

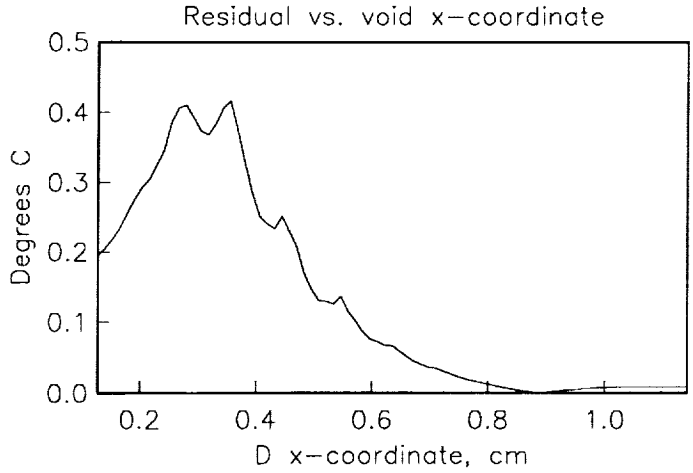

Figure 4: Functional $J(q)$ versus D x_1 coordinate.

This leads to the following strategy for locating a void, illustrated in Figure 5: Apply the heat source at a number of different points along the top the sample. For each different heating location, take the corresponding temperature measurements along the top of the sample. As one passes the heating source over a void it will be detected by a change in the temperature response. Suppose this occurs when the heating source has an x_1 coordinate equal to a. Then begin the optimization with initial guess $x_1 = a$ and x_2 and r anything reasonable. This should provide a reasonable approximation to the correct x_1 coordinate of the void; the initial guess at x_2 and r is much less crucial.

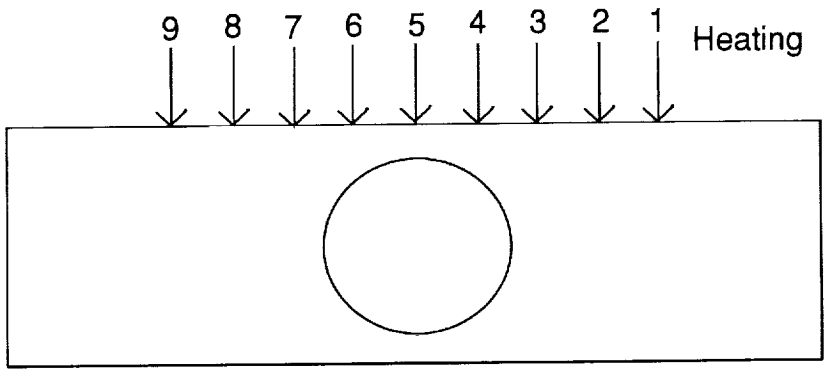

Figure 5: Strategy for applying heat sources.

5.4 Results

This procedure is illustrated by the graphs in Figure 6. The actual void D^* is located at (x_1, x_2) coordinates (0.77 cm, 0.24 cm) with radius 0.06 cm. A total of 9 point heating sources at 3 Hertz were applied on the sample top surface, equispaced, spanning one half of the sample length, with source 5 centered on the top surface. The graphs show the out of phase or imaginary portion of the temperature response for each source location. The temperature response changes most rapidly and peaks between heating locations 3 and 4. Contrast this to the temperature response when no void is present, shown in Figure 7; the response does not change, since nothing under the heating source changes as the source moves. A Levenberg-Marquardt algorithm implemented along the lines in [8] was used to recover an estimate of the void D^*, using only the peak temperature response data, heating sources 3 and 4. The initial guess at the x_1 coordinate was halfway between these sources at 0.75 cm. The x_2 and radius initial guesses were 0.16 cm and 0.1 cm, respectively. The optimization code converges to the correct void in 11 iterations, reducing the residual from 0.154 to less than 0.002. However, no noise was present.

As a more realistic example, we take the same geometry and void as the previous example but with 20 percent zero-mean gaussian noise (measure as percent of signal RMS value) added to the temperature response. The responses are shown in Figure 8. The largest response is for position 3. The data for heating positions 2, 3 and 4 were then used in the optimization with initial guess $x_1 = 0.79$ cm (the x_1 coordinate for source 3), $x_2 = 0.16$ cm

and $r = 0.1$ cm. The initial residual is 0.406. The optimization routine reduces this to 0.381 in 12 iterations. The final estimate for the void is $x_1 = 0.755$ cm, $x_2 = 0.22$ cm, $r = 0.067$ cm. The true void is shown as the solid outline in Figure 9 and the and recovered estimate as the dotted outline.

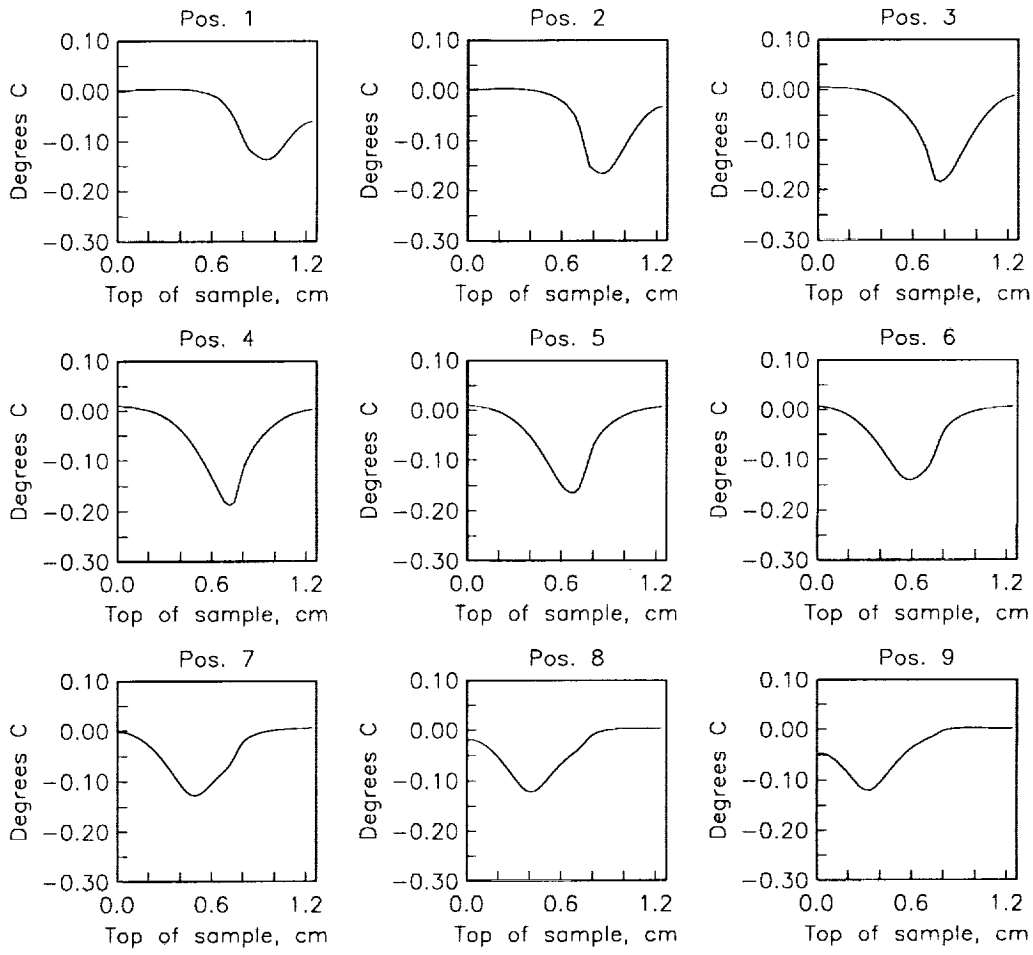

Figure 6: Out of phase temperature for varying heat source locations.

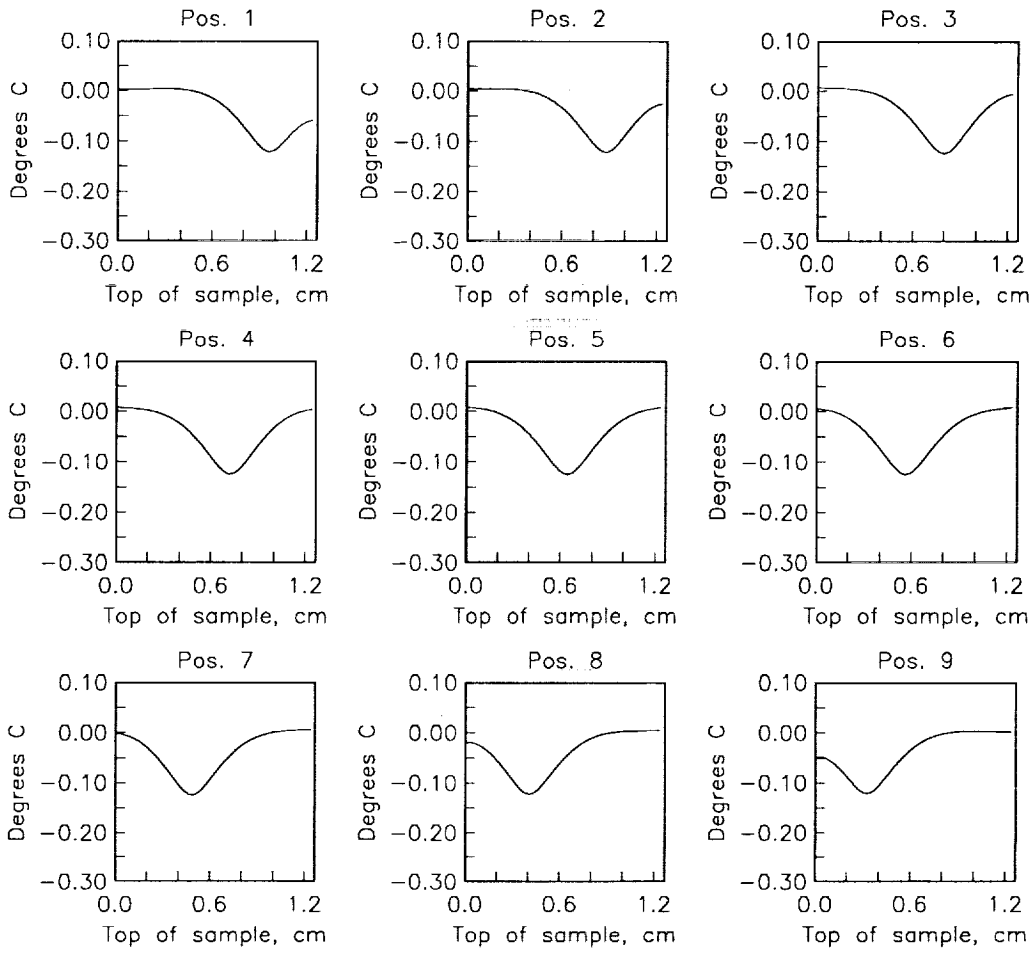

Figure 7: Out of phase temperature for varying heat source locations, no void.

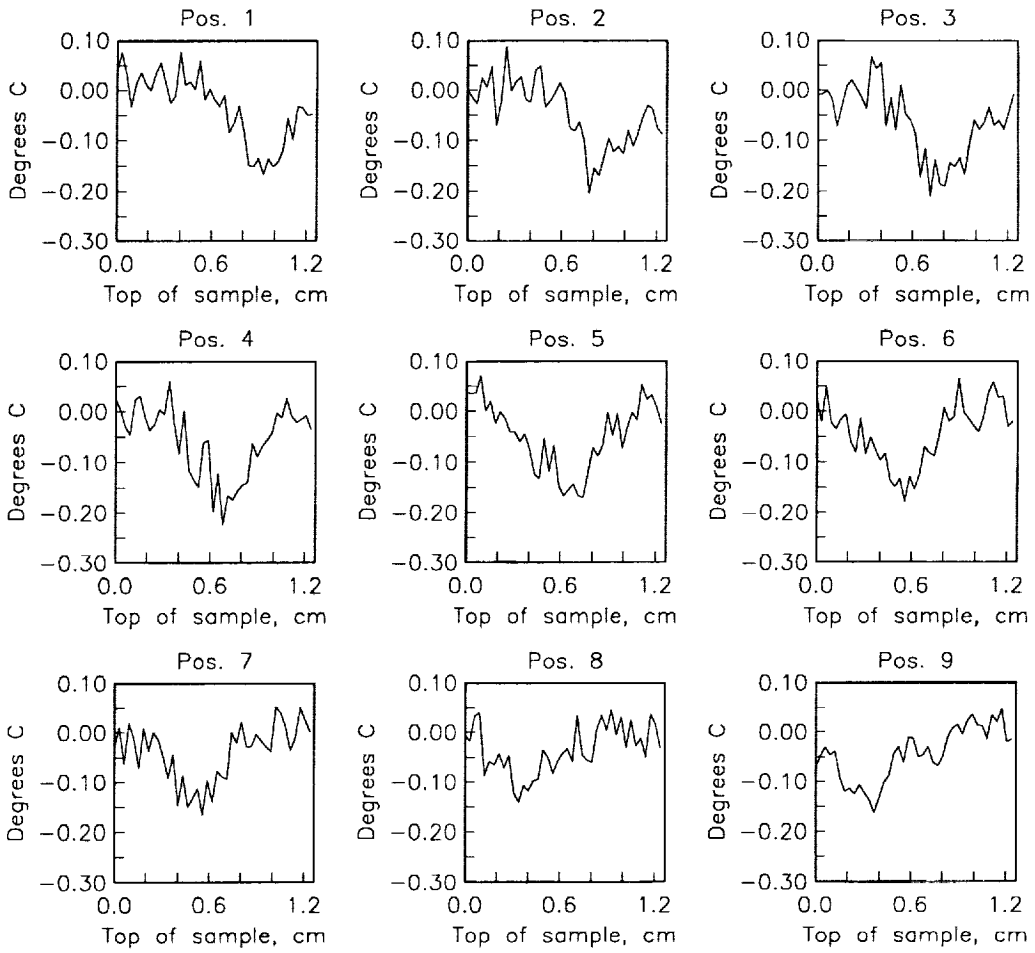

Figure 8: Out of phase temperature for varying heat source locations, 20 percent noise.

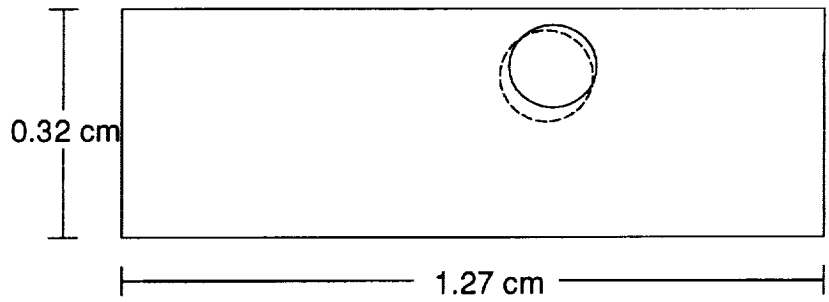

Figure 9: True and estimated void.

6 Conclusion

The problem of recovery a void in a material sample based on the sample's surface temperature response to external heating has been considered. Uniqueness and continuous dependence results have been shown, and an optimization based algorithm for recovering an estimate of the void has been demonstrated. Much of this work rests on reformulating the heat conduction problem as a boundary integral equation, which provides a means of rapidly solving the heat conduction equations. The algorithm was run for the simple case of a circular void and computationally generated data. This algorithm exhibits some of the problems that optimization approaches are heir to, specifically, the likelihood that a poor initial guess will not converge to a global minimum, and some strategies for overcoming this have been described.

Collection of actual data from a experimental setup at NASA Langley Research Center has already been performed. Preliminary analysis of this data shows good agreement with the heat conduction model and the ability to actually recover subsurface voids. The analysis of this experimental data will be reported elsewhere. Of interest for future research is a study of the sensitivity of this thermal technique, e.g., the size of voids which can be detected at various depths. Techniques for voids of different shapes (especially cracks or disbonds) should also be examined. The heat conduction model could also be improved; zero boundary flux away from the source becomes unrealistic at low frequencies. We would also like to pursue a full three-dimensional heat conduction model leading to a two-dimensional boundary integral formulation. Such a formulation would require a finite or boundary element technique for the numerical solution, rather than Nyström's method.

7 Acknowledgements

I would like to thank W.P. Winfree of the Nondestructive Sciences Evaluation Branch at NASA Langley Research Center and H. Thomas Banks of the Center for Scientific Computation at North Carolina State University for their helpful suggestions.

References

[1] Abramowitz, Milton and Irene Stegun, *Handbook of mathematical functions*, Applied Mathematics Series, vol. 55. Washington: National Bureau of Standards, 1964. Reprinted 1968 by Dover Publications, New York.

[2] Atkinson, K.E., *A survey of numerical methods for the solution of fredholm integral equations of the second kind*, SIAM, Philadelphia, PA, 1976.

[3] Banks, H.T. and F. Kojima, *Approximations techniques for domain identification in two-dimensional parabolic systems under boundary observations*, Proc. 20th IEEE CDC Conference, Los Angels, Dec. 9-11, (1987), pp.14411-1416.

[4] Banks, H.T. and F. Kojima, *Boundary shape identification problems in two-dimensional domains related to thermal testing of materials*, Quart. Appl. Math., Vol. 47 (1989), pp. 273-293.

[5] Banks, H.T., F. Kojima and W.P. Winfree, *Boundary estimation problems arising in thermal tomography*, Inverse Problems 6 (1990), pp. 897-922.

[6] Folland, Gerald B., *Introduction to partial differential equations.* Princeton, NJ: Princeton University Press, 1976.

[7] Kojima, F., *Identification of microscopic flaws arising in thermal tomography by domain decomposition method*, Proc. Computation and Control II, MSU (1990), Birkhäuser.

[8] More', J. *The Levenberg-Marquardt algorithm: implementation and theory.* Numerical Analysis (Edited by Watson, G.A.), pp. 105–116. *Lecture Notes in Math.* 630. Springer Verlag, 1977.

[9] Patel, P.M., S. K. Lau and D.P. Almond, *A review of image analysis techniques applied int transient thermographic nondestructive testing*, Nondestructive Testing and Evaluation, Vol. 6 (1992), pp.343-364.

[10] Radon, I., *Über die Randwetaufgaben beim logarithmischen Potential*, Sitzber. Akad. Wiss. Wien, 128 (1919), pp. 1123-1167.

REPORT DOCUMENTATION PAGE

Form Approved
OMB No. 0704-0188

Public reporting burden for this collection of information is estimated to average 1 hour per response, including the time for reviewing instructions, searching existing data sources, gathering and maintaining the data needed, and completing and reviewing the collection of information. Send comments regarding this burden estimate or any other aspect of this collection of information, including suggestions for reducing this burden, to Washington Headquarters Services, Directorate for Information Operations and Reports, 1215 Jefferson Davis Highway, Suite 1204, Arlington, VA 22202-4302, and to the Office of Management and Budget, Paperwork Reduction Project (0704-0188), Washington, DC 20503.

1. AGENCY USE ONLY (Leave blank)	2. REPORT DATE	3. REPORT TYPE AND DATES COVERED
	August 1992	Contractor Report

4. TITLE AND SUBTITLE
A BOUNDARY INTEGRAL METHOD FOR AN INVERSE PROBLEM IN THERMAL IMAGING

5. FUNDING NUMBERS
C NAS1-18605
C NAS1-19480
WU 505-90-52-01

6. AUTHOR(S)
Kurt Bryan

7. PERFORMING ORGANIZATION NAME(S) AND ADDRESS(ES)
Institute for Computer Applications in Science and Engineering
Mail Stop 132C, NASA Langley Research Center
Hampton, VA 23665-5225

8. PERFORMING ORGANIZATION REPORT NUMBER
ICASE Report No. 92-38

9. SPONSORING / MONITORING AGENCY NAME(S) AND ADDRESS(ES)
National Aeronautics and Space Administration
Langley Research Center
Hampton, VA 23665-5225

10. SPONSORING / MONITORING AGENCY REPORT NUMBER
NASA CR-189693
ICASE Report No. 92-38

11. SUPPLEMENTARY NOTES
Langley Technical Monitor: Michael F. Card
Final Report

Submitted to Journal of Mathematical Systems, Estimation and Control

12a. DISTRIBUTION / AVAILABILITY STATEMENT
Unclassified - Unlimited

Subject Category 64

12b. DISTRIBUTION CODE

13. ABSTRACT (Maximum 200 words)
This paper examines an inverse problem in thermal imaging, that of recovering a void in a material from its surface temperature response to external heating. Uniqueness and continuous dependence results for the inverse problem are demonstrated and a numerical method for its solution developed. This method is based on an optimization approach, coupled with a boundary integral equation formulation of the forward heat conduction problem. Some convergence results for the method are proved and several examples are presented using computationally generated data.

14. SUBJECT TERMS
inverse problem; thermal imaging; nondestructive evaluation

15. NUMBER OF PAGES
29

16. PRICE CODE
A03

17. SECURITY CLASSIFICATION OF REPORT	18. SECURITY CLASSIFICATION OF THIS PAGE	19. SECURITY CLASSIFICATION OF ABSTRACT	20. LIMITATION OF ABSTRACT
Unclassified	Unclassified		

NSN 7540-01-280-5500

Standard Form 298 (Rev. 2-89)
Prescribed by ANSI Std. Z39-18
298-102

NASA-Langley, 1992